Chapter 3
Evaluation of Heteroepitaxially Grown Semipolar {20-21} GaN on Patterned Sapphire Substrate

Yasuhiro Hashimoto, Masakazu Koyama, Takashi Inagaki, Keisuke Yamane, Narihito Okada and Kazuyuki Tadatomo

Abstract Semipolar {20-21} GaN layers were grown on {22-43} patterned sapphire substrates by metal–organic vapor phase epitaxy using a two-step growth method. We succeeded in suppressing $-c$-plane growth at growth temperatures of 1,000 and 900 °C for the first and second steps, respectively; the resulting structure exhibited a large reduction in the number of stacking faults upon optimizing the growth conditions. Photoluminescence measurements showed an increase in the near-band-edge emission and a decrease in deep-center emission when the two-step growth was performed at higher V/III ratio.

Keywords MOVPE • GaN • PSS • {20-21} • Stacking fault • PL

3.1 Introduction

GaN and other related semiconductor materials have been widely used in the fabrication of light-emitting diodes (LEDs), laser diodes (LDs), radio-frequency devices, and power devices. In general, commercially available LEDs and LDs are fabricated on a polar *c*-plane GaN. However, the quantum confined Stark effect (QCSE) due to polarization-induced strong internal electric fields inside *c*-plane InGaN/GaN multiple quantum wells causes the degradation of device performance. QCSE is reduced by using semipolar and nonpolar GaN substrates [1]. Most notably, the green LD has been realized by using a semipolar {20-21} GaN substrate [2], and improvements in the efficiency droop of LEDs for high injection currents have been achieved by using a semipolar {20-2-1} GaN substrate [3]. A nonpolar or semipolar GaN substrate is usually fabricated by slicing

---

Y. Hashimoto · M. Koyama · T. Inagaki · K. Yamane · N. Okada · K. Tadatomo (✉)
Graduate School of Science and Engineering, Yamaguchi University, Yamaguchi, Japan
e-mail: tadatomo@yamaguchi-u.ac.jp

R. Tutsch et al. (eds.), *Progress in Optomechatronic Technologies*,
Lecture Notes in Electrical Engineering 306, DOI: 10.1007/978-3-319-05711-8_3,

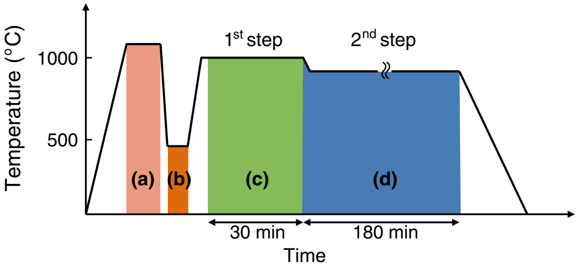

Fig. 3.1 Schematic of temperature profile for (**a**) thermal cleaning (**b**) growth of low-temperature GaN buffer layer **c** growth of GaN layer in first step, and (**d**) growth of GaN layer in second step. The V/III ratio was varied from 147 to 2,942

bulk *c*-plane GaN. Hence, large-sized semipolar {20-21} GaN substrates are not commercially available to grow the abovementioned device structures. Therefore, the fabrication of large-sized {20-21} GaN substrates on foreign substrates as well as *a*- [4], *m*- [5, 6], {10-1-3}, {11-22} [7], and {10-11} [8] is desirable. However, the use of {20-21} GaN templates on foreign substrates such as sapphire or silicon has not thus far been reported. We have previously reported the fabrication of a 2-inch-diameter {20-21} GaN layer on a patterned sapphire substrate (PSS) by using metal–organic vapor phase epitaxy (MOVPE) [9] and the subsequent fabrication of a 2-inch-diameter freestanding {20-21} GaN by using hydride vapor phase epitaxy (HVPE) [10]. In this light, previous studies have reported on the heteroepitaxial growth mode of semipolar GaN [11–13]. In order to obtain a high-crystalline-quality bulk {20-21} GaN substrate using the sapphire substrate, the crystalline quality of the {20-21} GaN layer is also important, and its growth mode should be investigated in detail. However, the growth mode of the {20-21} GaN layer has not thus far been investigated. In this work, we investigated the heteroepitaxial growth mode of a {20-21} GaN layer on PSS and the resulting crystalline quality of the {20-21} GaN layer.

3.2 Experimental Procedure

For the growth of the semipolar {20-21} GaN layer, we prepared a stripe-patterned {22-43} PSS with an SiO_2 mask. Stripe patterns were formed perpendicular to the *c*-axis of {22-43} sapphire by using conventional photolithography and inductively coupled plasma reactive ion etching (ICP-RIE). As a consequence, the stripe-patterned {22-43} PSS had a *c*-plane-like sapphire sidewall, because it is difficult to fabricate the exact *c*-plane sapphire sidewall using ICP-RIE. The depth and width of the grooves formed by etching were 1 and 3 μm, respectively. The period of the stripe pattern was 6 μm. The SiO_2 mask was deposited on the ridges to prevent the growth of GaN [13]. A {20-21} GaN layer was grown on the PSS by using MOVPE. Trimethylgallium (TMG) and ammonia (NH_3) were used as the sources of Ga and N, respectively. The carrier gas used was purified H_2. Figure 3.1 shows the temperature profile corresponding to the growth of a {20-21} GaN layer by MOVPE. A low-temperature GaN buffer layer was grown at 460 °C after thermal cleaning. Subsequently, a {20-21} GaN layer was grown by using a two-step growth method. The two-step growth method is useful to obtain perfectly coalesced GaN layers on the {22-43} PSS. Crystal growth was not interrupted between the first and second steps.

The {20-21} GaN layers were observed by scanning electron microscope (SEM) with an acceleration voltage of 5 kV. Stacking faults were characterized by photoluminescence (PL) measurements at 4 K by using a 14 mW, 325 nm He–Cd laser.

3.3 Results and Discussion

Firstly, we investigated the one-step growth of the semipolar {20-21} GaN layer on the {22-43} PSS [9]. The growth temperature and the V/III ratio were 1,000 °C and 294, respectively. This growth condition was optimized to obtain a selective area growth from the *c*-plane-like sapphire sidewall. Figure 3.2a, b show the cross-sectional SEM images of GaN layers grown for 60 and 300 min, respectively. The initial facet structure was composed of one $-c$-plane and two {10-11}, as shown in Fig. 3.2a. However, the GaN layers did not coalesce with each other after 300 min of growth. Furthermore, the $-c$-plane GaN was grown as shown in Fig. 3.2b, with the growth region exhibiting a large defect density [14, 15]. These defects were mainly characterized as the I_1 type of basal stacking faults (BSFs) by TEM observations. To mitigate these problems, we adopted the two-step growth method in this study.

The growth of the GaN layer at lower temperatures was effective in enhancing the growth rate toward the $+c$-direction such that the $+c$ facet structure shown in Fig. 3.2b disappeared [16]. Therefore, the two-step growth method was adopted to obtain coalesced continuous GaN layers. The growth temperatures of the first and second steps were 1,000 and 900 °C, respectively. The V/III ratio was maintained at 294 during the two-step growth process. The first step initiates the growth of the GaN nucleus (Fig. 3.2a), and the second step leads to coalescence of the GaN layers. Figure 3.3 shows a cross-sectional SEM image of a perfectly coalesced GaN layer achieved by the two-step process. Triangular voids surrounded by the {10-11} GaN, $-c$-plane GaN, and {22-43} sapphire surface were formed. The GaN-layer surfaces consisted of *m*-plane and {10-11} facets. The width of the GaN-layer growth region toward the $-c$-direction was approximately 100 nm.

Next, we investigated the temperature dependence of the growth rate for the second step. Figure 3.4a, b show cross-sectional SEM images of the GaN layers grown at 900 and 925 °C, respectively, in the second stage. Both GaN layers were perfectly coalesced. However, for the growth temperature of 925 °C, a large GaN growth region toward the $-c$-direction was observed. The width of this region was greater than 1,000 nm. We found that the optimization of growth temperature was essential to form a continuous GaN layer and to suppress GaN growth toward the—*c*-direction.

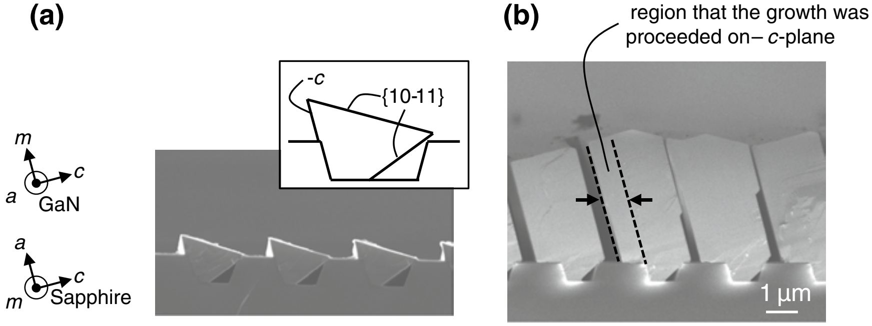

Fig. 3.2 Cross-sectional SEM images of semipolar {20-21} GaN layers grown (**a**) in initial stage and (**b**) for 5 h by one-step growth

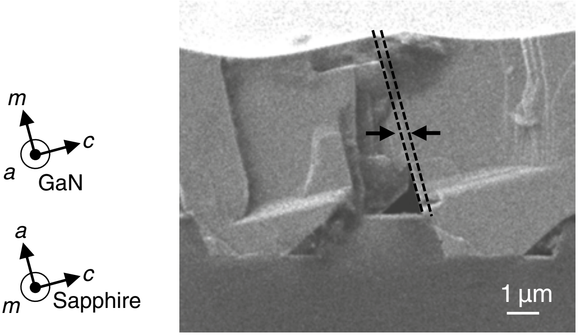

Fig. 3.3 Cross-sectional SEM image of semipolar {20-21} GaN layer grown by two-step method. Growth temperatures of first step/second step were 1,000 °C/900 °C. Dashed lines indicate the region of GaN-layer growth toward the—*c*-direction

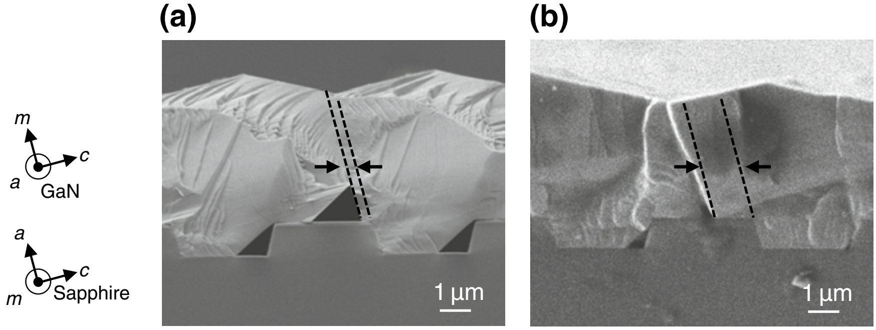

Fig. 3.4 Cross-sectional SEM images of semipolar {20-21} GaN layers grown by using two-step growth method. The growth temperatures of the first step/second step were (**a**) 1,025 °C/900 °C and (**b**) 1,025 °C/925 °C. Dashed lines indicate the region of GaN growth toward the—*c*-direction

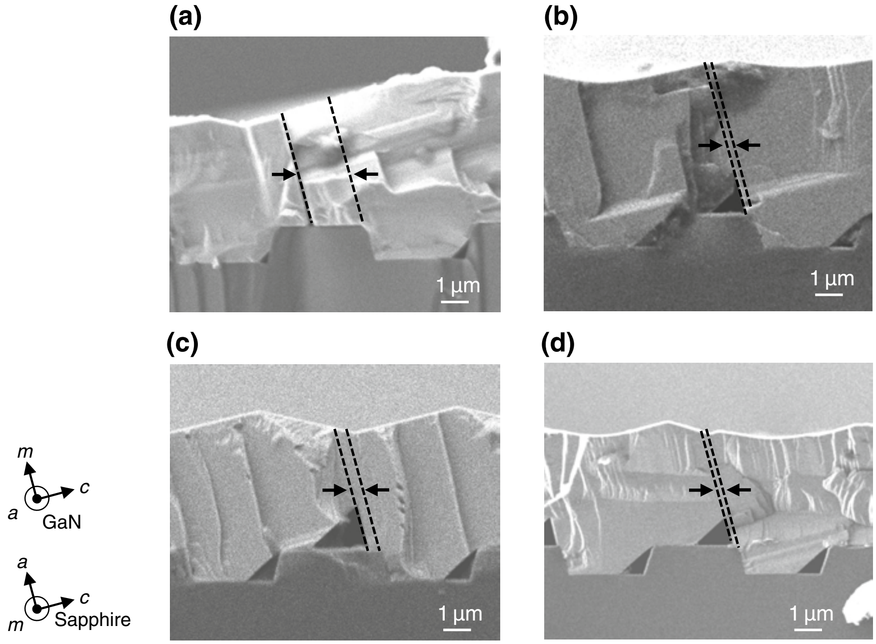

Fig. 3.5 Cross-sectional SEM images of semipolar {20-21} GaN layers grown by two-step growth method. The V/III ratios were (**a**) 147 (**b**) 294 (**c**) 882, and (**d**) 2,942. The growth temperatures of the first step/second step were fixed at 1,000 °C/900 °C, respectively. Dashed lines indicate the regions of GaN-layer growth toward the—*c*-direction

The choice of the V/III ratio also affects the growth mode and crystalline quality of GaN. Because the GaN surface along the $+c$-plane is terminated by Ga atoms (Ga-polar) and that along the $-c$-plane is terminated by N atoms (N-polar), the growth of GaN along the $-c$-plane GaN was suppressed at low values of the V/III ratio [14]. Finally, therefore, we investigated the effect of the V/III ratio on the growth mode of {20-21} GaN. The growth temperatures of the first and second steps were fixed at 1,000 and 900 °C, respectively. The V/III ratio was varied as 147, 294, 882, and 2,942. Figure 3.5 shows the cross-sectional SEM images of the GaN layers grown at different V/III ratio. The width of the GaN-layer growth region toward the $-c$-direction was approximately 200 nm when the V/III ratio was greater than 294. Despite the lowest V/III ratio of 147, the GaN-layer-width toward the $-c$-direction was greater than 1,500 nm. Although the reason underlying this phenomenon is unclear and under investigation, we speculate that the generation of many facet structures such as $-c$, $+c$, m, and {10-11} planes can complicate the growth mode.

Figure 3.6 shows the near-band-edge (NBE) emission intensity and deep-center emission (yellow luminescence) intensity of the grown GaN layers as a function of the V/III ratio when measured at 4 K. The NBE emission was enhanced drastically with increase in the V/III ratio. The intensity of NBE emission of the sample

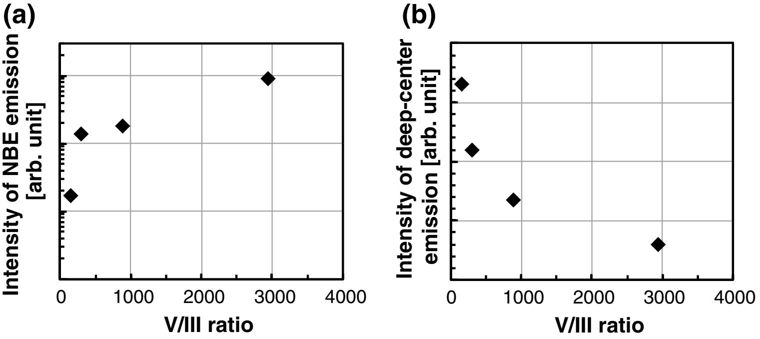

Fig. 3.6 PL intensity of (**a**) NBE emission and (**b**) deep-center emission as function of V/III ratio

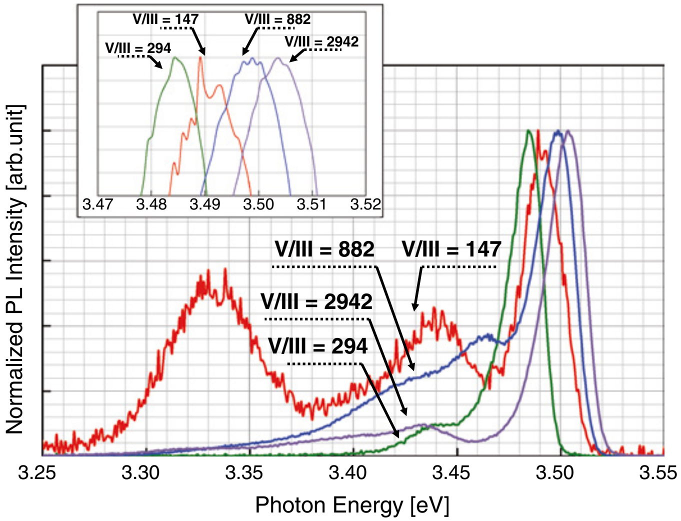

Fig. 3.7 PL spectra of semipolar {20-21} GaN layers grown at various V/III ratio at 4 K. Inset shows magnification of the spectra around the range of NBE emissions

grown with the V/III ratio of 2,942 was approximately 50 times greater than that grown at a V/III ratio of 147. The deep-center emission decreased with increase in the V/III ratio, as shown in Fig. 3.6b. We speculate that N vacancies are suppressed at large V/III ratio.

Figure 3.7 shows the PL spectra of semipolar {20-21} GaN layers grown at various V/III ratios measured at 4 K. A peak at around 3.49 eV representing NBE emission was observed for the {20-21} GaN layers grown on the {22-43} PSS. BSFs and prismatic stacking faults (PSFs) were responsible for emission at energies of approximately 3.44 and 3.33 eV, respectively [17]. The I_1 type of BSFs with the lowest formation energies [18] were observed in all samples. The GaN layer with strong emission corresponding to BSFs exhibited a large GaN-layer growth region toward the $-c$-direction. When the V/III ratio was 147, a strong emission corresponding to PSFs was observed. The NBE emission peaks exhibited a gradual shift to the high-energy side with increasing V/III ratio, as shown in inset of Fig. 3.7. The slight difference was attributed to the variation in compressive stress in the sample structures. A large V/III ratio was necessary to grow GaN layers with a reduced concentration of deep-center defects, such as N vacancies, and without lattice relaxation. High-quality template is essential for the high-efficiency devices. We expect that semipolar GaN template with low defect density realize more efficient and cheap as light sources for optoelectronic devices.

3.4 Summary

In conclusion, we achieved the heteroepitaxial growth of semipolar {20-21} GaN on {22-43} PSS by using MOVPE, and we investigated the GaN growth mode of these samples. We succeeded in suppressing growth toward the $-c$-direction at growth temperatures of 1,000 and 900 °C for the first step and the second step, respectively; this resulted in a large reduction in the formation of stacking faults. The PL measurements showed an increase in NBE emission and a decrease in deep-center emission when the two-step growth was performed at higher V/III ratio. We believe that our study will contribute to realize more efficient and cheap light sources for optoelectronic devices.

Acknowledgments This work was partly supported by the "Regional Innovation Cluster Program" (Global Type), and a Grant-in-Aid for Young Scientists B # 24,760,012 funded by the Ministry of Education, Culture, Sports, Science and Technology, Japan

References

1. Funato M, Ueda M, Kawakami Y, Nakamura Y, Kosugi T, Takahashi M, Mukai T (2006) Blue, green, and amber InGaN/GaN light-emitting diodes on semipolar {11-22} GaN bulk substrates. Jpn J Appl Phys 45:L659
2. Enya Y, Yoshizumi Y, Kyono T, Akita K, Ueno M, Adachi M, Sumitomo T, Tokuyama S, Ikegami T, Katayama K, Nakamura T (2009) 531 nm green lasing of InGaN based laser diodes on semi-polar {20-21} free-standing GaN substrates. Appl Phys Express 2:082101
3. Zhao Y, Tanaka S, Pan CC, Fujito K, Feezell D, Speck JS, DenBaars SP, Nakamura S (2011) High-power blue-violet semipolar (20-2-1) InGaN/GaN light-emitting diodes with low efficiency droop at 200 A/cm^2. Appl Phys Express 4:082104
4. Sasaki T, Zembutsu S (1987) Substrateorientation dependence of GaN single-crystal films grown by metalorganic vapor-phase epitaxy. J Appl Phys 61:2533
5. Waltereit P, Brandt O, Trampert A, Grahn HT, Menniger J, Ramsteiner M., Reiche M, Ploog KH (2000) Nitride semiconductors free of electrostatic fields for efficient white light-emitting diodes. Nature 406:865 (London)

6. Armitage R, Hirayama H (2008) M-plane GaN grown on m-sapphire by metalorganic vapor phase epitaxy. Appl Phys Lett 92:092121
7. Baker TJ, Haskell BA, Wu F, Speck JS, Nakamura S (2006) Characterization of planar semipolar gallium nitride films on sapphire substrates. Jpn J Appl Phys 45:L154
8. Baker TJ, Haskell BA, Wu F, Fini PT, Speck JS, Nakamura S (2005) Characterization of planar semipolar gallium nitride films on spinel substrates. Jpn J Appl Phys 44:L920
9. Okada N, Oshita H, Yamane K, Tadatomo K (2011) High-quality {20-21} GaN layers on patterned sapphire substrate with wide-terrace. Appl Phys Lett 99:242103
10. Yamane K, Ueno M, Uchida K, Furuya H, Okada N, Tadatomo K (2012) Reduction in dislocation density of semipolar GaN layers on patterned sapphire substrates by hydride vapor phase epitaxy. Appl Phys Express 5:095503
11. Schwaiger S, Argut I, Wunderer T, Rosch R, Lipski F, Biskupek J, Kaiser U, Scholz F (2010) Planar semipolar(10-11) GaN on (11-23) sapphire. Appl Phys Lett 96:231905
12. Honda Y, Kawaguchi Y, Ohtake Y, Tanaka S, Yamaguchi M, Sawaki N (2001) Selective area growth of GaN microstructures on patterned (111) and (001) Si substrates. J Cryst Growth 230:346
13. Okada N, Kurisu A, Murakami K, Tadatomo K (2009) Growth of Semipolar (11–22) GaN layer by controlling anisotropic growth rates in r-plane patterned sapphire substrate. Appl Phys Express 2:091001
14. Yamane K, Inagaki T, Hashimoto Y, Koyama M, Okada N, Tadatomo K (2014) Characterization of structural defects in semipolar {20-21} GaN layers grown on {22-43} patterned sapphire substrates. Jpn J Appl Phys 53:035502
15. Kawashima T, Nagai T, Iida D, Miura A, Okadome Y, Tsuchiya Y, Iwaya M, Kamiyama S, Amano H, Akasaki I (2007) Reduction in defect density over whole area of (1-100) m-plane GaN using one-sidewall seeded epitaxial lateral overgrowth. Phys Status Solidi B 244:1848
16. Miyake H, Motogaito A, Hiramatsu K (1999) Effects of reactor pressure on epitaxial lateral overgrowth of GaN via low-pressure metalorganic vapor phase epitaxy. Jpn J Appl Phys 38:L1000
17. Mei J, Srinivasan S, Liu R, Ponce FA, Narukawa Y, Mukai T (2006) Prismatic stacking faults in epitaxially laterally overgrown GaN. Appl Phys Lett 88:141912
18. Stampfl C, Van de Walle CG (1998) Energetics and electronic structure of stacking faults in AlN, GaN, and InN. Phys Rev B 57:R15052